

Applying Fourier numerical analysis to determination of tensor elements of the deformations of seed covers

BOŻENA GŁADYSZEWSKA¹, DARIUSZ CHOCYK²

¹Department of Physics, Agriculture University of Lublin, ul. Akademicka 13, 20-950 Lublin, Poland, e-mail: broz@ursus.ar.lublin.pl

²Lublin University of Technology, ul. Nadbystrzycka 38, 20-618 Lublin, Poland

A video-extensometry method for studying the mechanical properties of seed covers is presented. Young's modulus and Poisson's ratio for the material tested, *i.e.*, seed covers of dried broad beans (*Vicia faba*) are determined. A microscopic image of thin film gold nets (42 and 162 μm thick) deposited on sample surface was transferred through a camera to computer memory which carried out the analysis of changes occurring in the course of sample tension. Fourier's numerical analysis was applied to determine tensor elements of deformations of the materials under study. The method is characterized by high measuring accuracy. Another advantage lies in its insensibility to additional boundary effects, which could occur in the vicinity of sample clips.

Keywords: Stress measurement, Fourier analysis, Young's modulus, Poisson's ratio.

1. Introduction

Production of seeds of legumes is becoming more and more mechanized. A multiphase crop is not much frequently used as it has been replaced with mechanized harvester one. When being cropped seeds are subject to large mechanical loads due to which destructive strains may occur [1]–[3]. Seed covers can be destroyed also in the course of the process of drying [4], [5]. To find reasons for that, knowledge of the physical properties of seed covers is necessary, particularly Young's modulus and Poisson's ratio. Knowledge of mechanisms responsible for causing seed damage is essential to restrict seed material losses and improve its quality and commercial value.

The grid method is one of the most powerful tools for optical strain measurement [6]. Optical diffraction pattern of the grid is then studied during a test [7]. The spatial frequency is observed during an experiment, and changes in frequency are detected and directly related to strain. Some extensions of this procedure were presented and used for studying mechanical properties of different kinds of materials

[8]–[11]. Using an optoelectronic device an automatic calculation of strain distribution was also possible [12]. Due to the recent development of CCD cameras these methods have been revived [6], [13]–[16].

2. Method

Determination of Young's modulus E and Poisson's ratio ν for thin-bedded seed covers in the applied method is brought to define deformations of surface elements of an object under study that is subject to mono-axial tension. In such a case, it is sufficient to determine the state of deformation in tension plane. To that end, changes in the pattern of net lines deposited on the surface studied are observed by CCD camera. The simplest pattern of such lines is a square net. Under the action of applied force, the net deforms and turns to parallelepiped one. However, it is not vital that direction of force applied to non-deformed net be considered further.

In order to determine the parameters of a deformed net in the image acquired (Fig. 1a), a two-dimensional Fourier transform (Fig. 1b) is used. If the image is

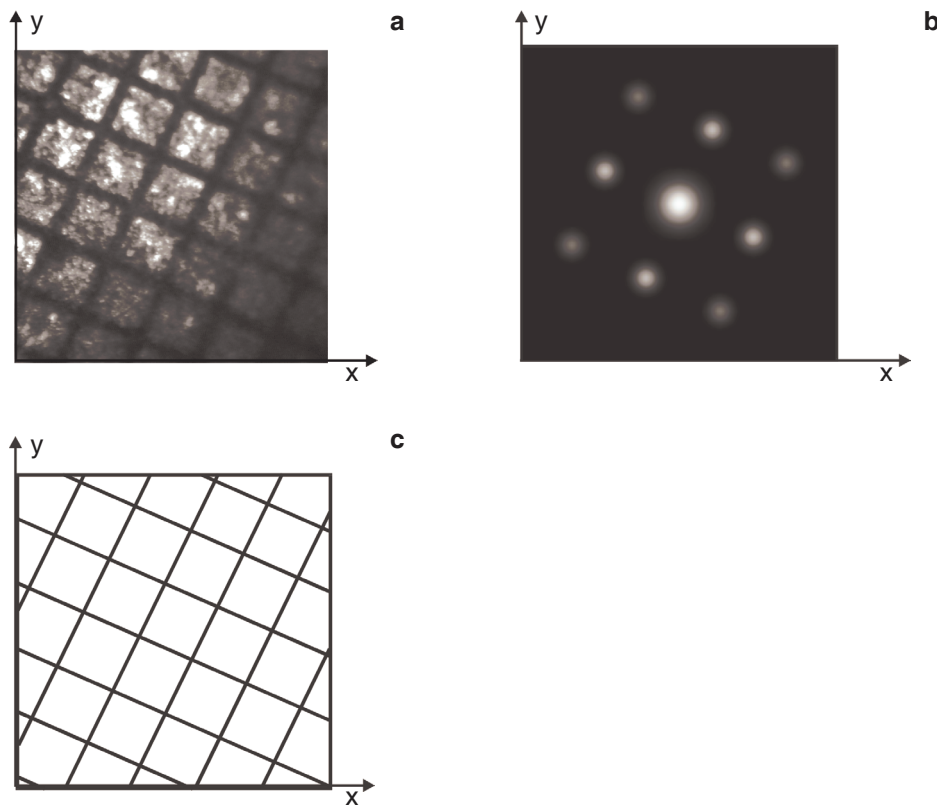


Fig. 1. Diagram of determination of mean deformed net: **a** – real image of deformed net, **b** – 2D Fourier transform of deformed net, **c** – mean deformed net.

shown as a square table $x(n, m)$ (representing intensity of the image point), a discrete two-dimensional Fourier transform is calculated using the following formula [17]:

$$X(k, l) = \sum_{n=0}^{N-1} \sum_{m=0}^{N-1} x(n, m) \exp\left[-\frac{2\pi i}{N} (km + ln)\right] \quad (1)$$

where N is the number of image points in perpendicular directions. Distances between maxima in the calculated table $X(k, l)$ show the frequency of occurrence of lines in two mutually perpendicular directions in the real image. Excluding ideal cases, distances between lines after sample intensity, are not equal and the distance between peaks stands for a certain value of frequency mean. These frequency means help to determine proper distances in a real deformed net and also proper angles with reference to one of the directions of lines before deformation.

In order to determine the position of maxima, a weighted mean of position is calculated for each peak. The value of discrete two-dimensional Fourier transform $X(k, l)$ is a weight for point correspondence to indexes k and l . The accuracy of peak position depends on the resolution of CCD camera. Considering a homogeneous state of deformation in the whole system, a mean deformed net (Fig. 1c) is made, which is described by the distances between lines and proper angles. The pattern is shown in Fig. 1. Knowing the parameters of a deformed net allows to determine proper deformations on surface.

If any point of coordinates (x, y) inside a square of a side p before deformation is considered, its coordinates after deformation have the following values (Fig. 2):

$$x' = \frac{a_1}{p} \cos(\alpha_1)x + \frac{a_2}{p} \cos(\alpha_2)y, \quad (2)$$

$$y' = \frac{a_1}{p} \sin(\alpha_1)x + \frac{a_2}{p} \sin(\alpha_2)y$$

where a_1 and a_2 are the sides of acquired parallepiped, respectively, and angles α_1 and α_2 are the inclination angles of these sides relative to the directions of the side before deformation. As mentioned above, parameters a_1 , a_2 , α_1 and α_2 are directly determined by means of the image of Fourier analysis after deformation.

Transformation of the co-ordinates of a point of deforming system allows us to determine a displacement vectors:

$$\mathbf{u} = \left[\frac{a_1}{p} \cos(\alpha_1) - 1 \right] x + \frac{a_2}{p} \cos(\alpha_2) y, \quad (3)$$

$$\mathbf{v} = \frac{a_1}{p} \sin(\alpha_1) x + \left[\frac{a_2}{p} \sin(\alpha_2) - 1 \right] y$$

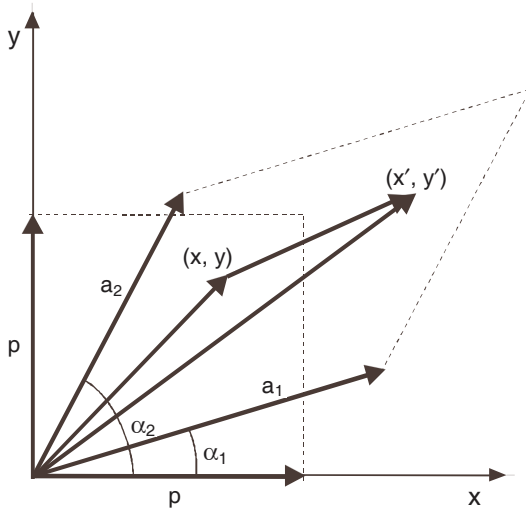


Fig. 2. Coordinates of a point before and after deformation.

which makes it possible to determine tensor deformation elements at a given point. To assume that deformations are homogeneous in the whole system, one can presume that they are the same at each point and the right Cauchy–Green deformation tensor elements depend only on mean values of a deformed net [6], [18]

$$T^{(d)} = \begin{bmatrix} \left(\frac{a_1}{p}\right)^2 & \frac{a_1 a_2}{p^2} \cos(\alpha_2 - \alpha_1) \\ \frac{a_1 a_2}{p^2} \cos(\alpha_2 - \alpha_1) & \left(\frac{a_2}{p}\right)^2 \end{bmatrix}. \quad (4)$$

The elements of this tensor define deformations ε_{ij} to coordinate system with reference to the net before deformation. However, deformations in coordinate system rotated at power angle φ can be formulated by [19]:

$$\varepsilon'_x = \frac{\varepsilon_x + \varepsilon_y}{2} + \frac{\varepsilon_x - \varepsilon_y}{2} \cos 2\varphi + \frac{\varepsilon_{xy}}{2} \sin 2\varphi, \quad (5a)$$

$$\varepsilon'_{xy} = -\frac{\varepsilon_x - \varepsilon_y}{2} \sin 2\varphi + \frac{\varepsilon_{xy}}{2} \cos 2\varphi, \quad (5b)$$

$$\varepsilon'_y = \frac{\varepsilon_x + \varepsilon_y}{2} - \frac{\varepsilon_x - \varepsilon_y}{2} \cos 2\varphi - \frac{\varepsilon_{xy}}{2} \sin 2\varphi. \quad (5c)$$

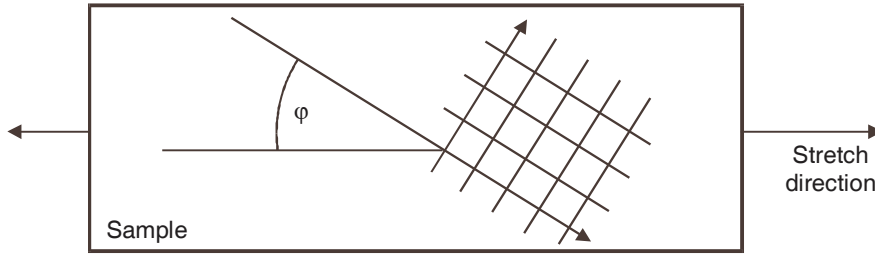


Fig. 3. Mutual orientation of sample and deposited gold net.

When two axes of the rotated system overlap with main axes, deformations in these directions have extreme values and deformation ε'_{xy} equals zero. Hence, the inclination angle of main deformation axes to original coordinate system can be determined (see Fig. 3)

$$\tan 2\varphi = \frac{\varepsilon_{xy}}{\varepsilon_x - \varepsilon_y}. \quad (6)$$

Knowledge of the power angle φ and deformations in the rotated system to system of main axes facilitates calculation of main deformations ($\varepsilon'_x, \varepsilon'_y$) which overlap with directions of main stresses in isotropic materials. Hence, Young's modulus and Poisson's ratio in demand are formulated as follows:

$$E = \frac{\sigma}{\varepsilon'_x}, \quad (7)$$

$$\nu = -\frac{\varepsilon'_y}{\varepsilon'_x}. \quad (8)$$

3. Experimental

In order to check the usefulness of Fourier numerical analysis in defining tensor deformation elements and Young's modulus and Poisson's ratio of seed covers, dried broad bean seeds (*Vicia faba*) were chosen for analysis. Samples of approximately 25 mm in length and approximately 8 mm in width were cut out of seed covers. Sample thickness was determined using micrometer screw. Then gold net was deposited on sample surface by means of cathode sputtering method with a mask properly prepared (typical masks applied in electron microscopy were used). The thickness of the gold layer did not exceed 200 nm, so it did not change mechanical properties of the sample. Figure 4 shows an example of sample with deposited gold layer (net). Nets of two

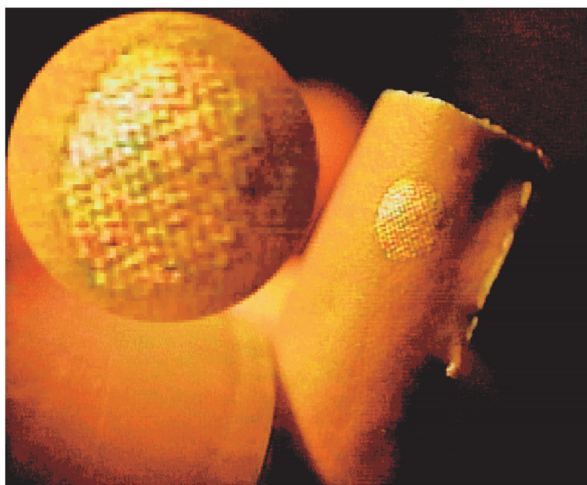


Fig. 4. General appearance of the sample under study.

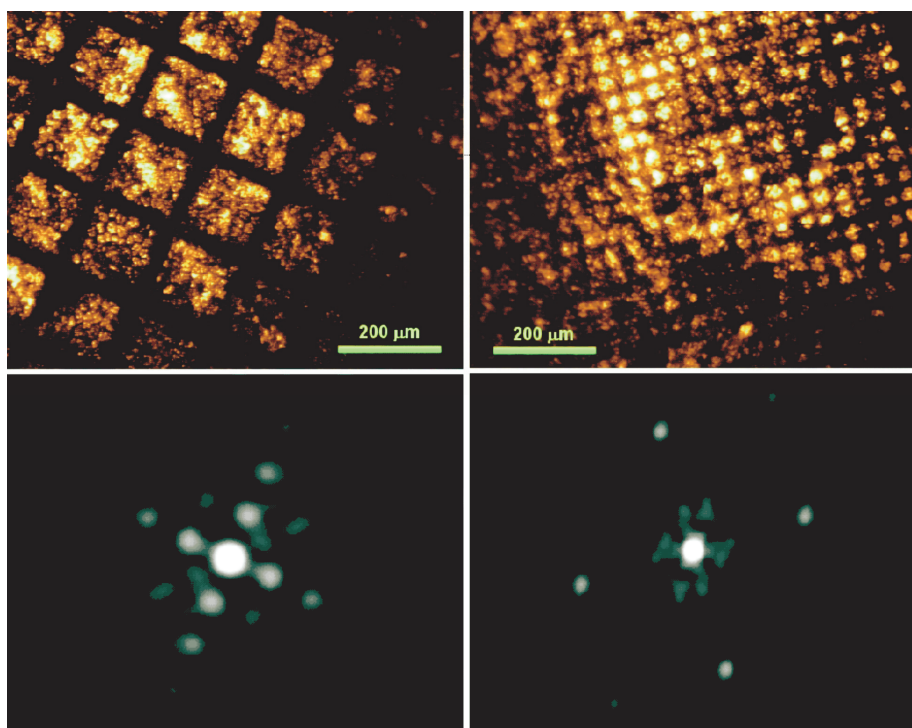


Fig. 5. Two different gold nets deposited on the samples and the images corresponding to them acquired with application of two-dimensional Fourier transform.

different periods (165 and 42 μm) were used. The sample thus prepared was installed in Microtest stress tester made by Deben Company, Ltd. Microscopic image of nets was transferred using a camera to computer memory which carried out the analysis of changes occurring during sample tension. Two applied nets and Fourier decompositions in non-stressed state corresponding to them are presented in Fig. 5. Values of ε'_x and ε'_y were determined using the equations given above. Knowing cross-sectional area of a certain sample and value of tensile force, a stress value σ was calculated. On this basis values of Young's modulus E and Poisson's ratio ν were determined. Below we present results obtained for two samples To4 and To5 (dimensions, length \times width \times thickness, 20 \times 8.5 \times 0.20 mm and 21 \times 7.25 \times 0.32 mm, respectively).

4. Results

Figure 6 shows an example of a graph of tensile force dependence on gain in distance between the gripping clips. Strong sample deformation occurring when there was no change of tensile force (approx. 10 N) might suggest the start of sample plastic deformation and an approaching moment of achieving critical values of intensity. In fact, an increase in the distance between the gripping clips ranging from 0.1 to 1.1 mm results from the slipping of sample edge out of tester clips. After the clips were clenched again, the sample was subjected to other deformations until critical value of tensile force 30 N was reached. It is obvious that relying on relations of this type would lead to incorrect results. The method suggested in the report is devoid of the above errors. Therefore, regardless of the total moving gripping clips, information on tensile force refers directly to sample deformation described by a change in position of Fourier peaks.

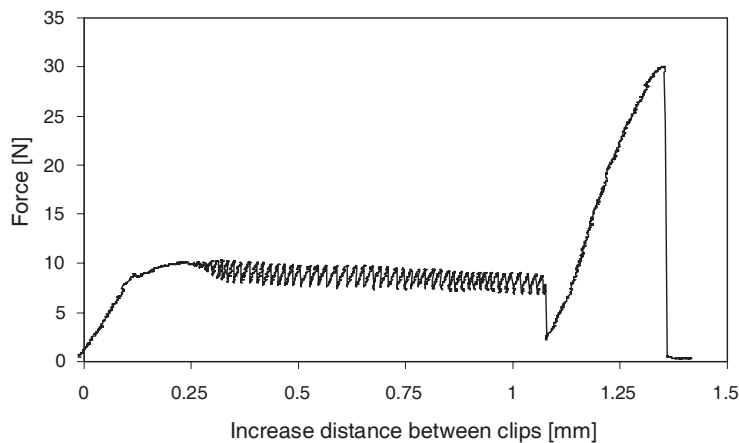


Fig. 6. Example of graph of tensile force dependence on an increase in distance between the gripping clips.

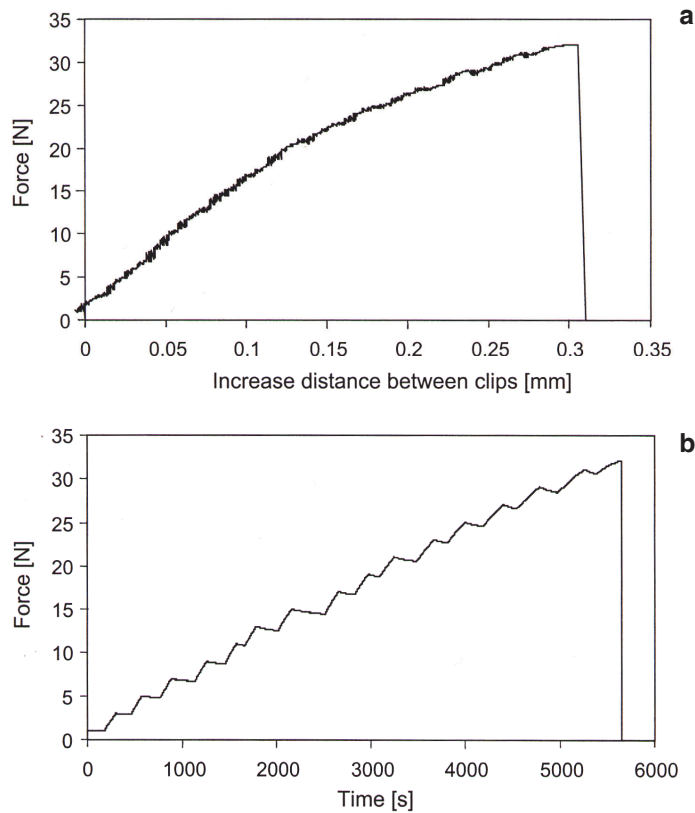


Fig. 7. Example of graph of tensile force dependence on an increase in distance between the gripping clips (a). The same relation is also shown as a function of time (b). Plastic nature of deformed sample is visible, change of threshold inclination, particularly for force range of over 15 N.

A similar relation (in the case of tester clips gripped properly) is shown in Fig. 7a, b, where a change in tensile force is also depicted as a function of time. To begin with initial value of tensile force 1 N, further sample tension was interrupted for approx. 200 s. The procedure was repeated when the force was increased by 2 N. Upper reaching 32 N, the sample was broken off. Taking sample sizes into consideration, the resistance threshold amounted to approx. 14 MPa. A plastic nature of sample deformation is visible, particularly for force range over 15 N. In periods of keeping tester clips at a stable distance, the value of force dropped clearly. Also in this case, the data need to be interpreted carefully since relations obtained include the total sample length. What really matters is boundary effects that occur in the vicinity of extensometer tester clips. They bring about an additional measuring error which causes quicker occurrence of plastic nature of deformations.

Figure 8 shows results of the video-extensometer application used to define Young's modulus of the two examples of samples (marked as To4 and To5, respectively) in the range of their elastic deformation. Young's modulus $E = 1.73$ GPa

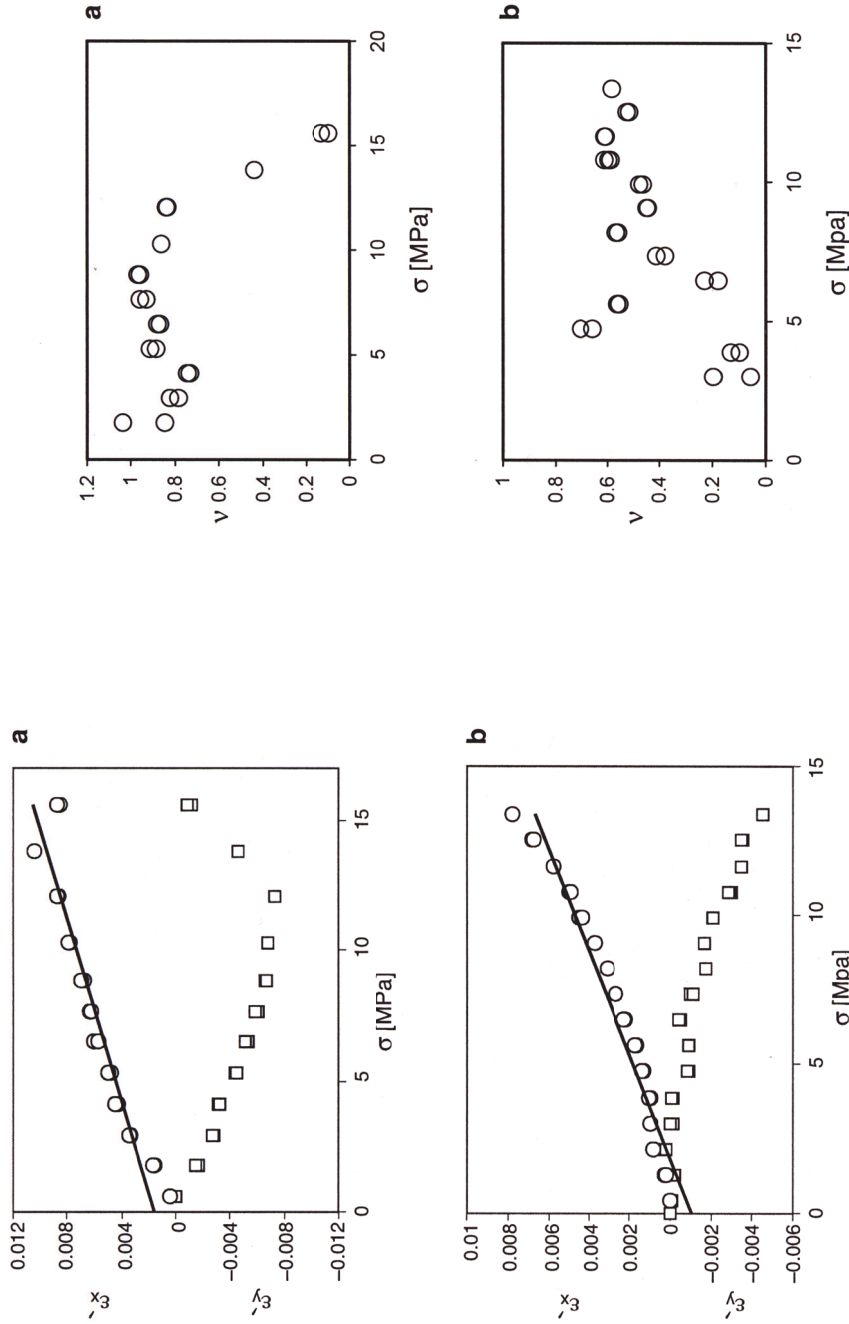


Fig. 8. Relations of $\varepsilon'_x(\sigma)$ and $\varepsilon'_y(\sigma)$ prepared for samples To4 (a) and To5 (b). Young's modulus determined with inclination angle of straight line inscribed in relation of $\varepsilon'_x(\sigma)$ amounts to $E = 1.73$ GPa for two samples.

Fig. 9. Dependence of Poisson's ratio ν on temporary intensity value prepared for samples To4 (a) and To5 (b). A large scatter of values is seen which shows a change occurrence under the action of tensile force.

for both samples To4 and To5 is calculated with inclination angle of straight line inscribed into ϵ'_x relation. Very similar results were also obtained with other samples not included in this work.

However, a very large scatter of values is visible on graphs of Poisson's ratio dependence on temporary intensity value (Fig. 9) which shows occurrence of crosswise changes in sample under the action of tensile force activity. The changes can be attributed to progressive lengthwise bedding of cover fibers. Explanation of this effect will be possible after more complex research in different directions have been made.

5. Conclusions

The method presented here based on Fourier numerical analysis to define tensor elements of deformations of the material under study is characterized by much greater precision of measurements. The method makes then direct connection of tensile force value with acquired deformation possible. It is not reasonable as regards boundary effects to introduce an additional error (e.g., influence of tester clips).

Results from research into seed covers of dried broad bean seeds (*Vicia faba*) should be considered an example of broader application of this method. Knowing the mechanisms which bring about damage to seeds is essential to restrict seed material losses and improve their quality and value. Using the method proposed, research is being currently performed also for other materials, the results of which will be published soon.

Acknowledgments – The authors thank sincerely Pascale Villain and Philippe Goudeau from Laboratoire de Metallurgie Physique in Poitiers – Futuroscope (France) for aid in making measurements.

References

- [1] PICKETT L.K., Trans. Am. Soc. Agric. Eng. **16** (1973), 1047.
- [2] SINGH B., LINVILL D.E., Trans. Am. Soc. Agric. Eng. **20** (1977), 226.
- [3] DOBRZAŃSKI B., RYBCZYŃSKI R., *Mechanical properties of leguminoous seeds*, [In] *Proceedings of Agricultural and Biological Engineering Conference*, UK, Newcastle 1995, p. 1.
- [4] HENDERSON S.M., PABIS S., J. Agric. Engng. Res. **7** (1962) 85.
- [5] PABIS S., JAYAS D.S., CENKOWSKI S., *Grain Drying: Theory and Practice*, Wiley, New York 1998.
- [6] DUPRE J.-C., BREMAND F., LAGARDE F., Opt. Lasers Eng. **18** (1993), 159.
- [7] BELL J.F., *Diffraction grating strain gage*, [In] *Proceedings of the Society for Experimental Stress Analysis*, Vol. 17, No. 1-2, (1959/60), p. 51.
- [8] DOUGLAS R.A., AKKOC C., PUGH C.E., Exp. Mech. **5** (1965), 233.
- [9] SHARPE W.N., Exp. Mech. **8** (1968), 164.
- [10] PRYOR T.R., NORTH W.P.T., Exp. Mech. **11** (1971), 565.
- [11] BOONE P., Exp. Mech. **11** (1971), 481.
- [12] SEVENHUIJSEN P.J., Berichte VDI **313** (1978), 143.
- [13] BREQUE C., BREMAND F., DUPRE J.-C., Proc. SPIE **4317** (2001), 463.

- [14] MOULDER J.C., READ D.T., CARDENAS-GARCIA J.F., *New video-optical method for whole-field strain measurements*, [In] *Proceedings of the SEM Spring Conference on Experimental Mechanics*, New Orleans 1986, p. 700.
- [15] BREMAND F., DUPRE J.-C., LAGARDE A., *Eur. J. Mech. A: Solids* **11** (1992), 349.
- [16] AUVERGNE M., PINAULT S., TERRILLON T., *Caracterisation des lois de comportement des materiaux biologiques*, These DEA, Laboratoire de Mecaniques des Solides, Universite de Poitiers IUP3 GM 2001.
- [17] OPPENHEIM A.V., SCHAFER R.W., *Digital Signal Processing*, Prentice Hall, Englewood Cliffs, New York 1975, pp. 320–321.
- [18] LUBARDA V.A., *Elastoplasticity Theory*, CRC Press, Boca Raton, London, New York, Washington, D.C. 2002.
- [19] TIMOSHENKO S., GOODIER J.N., *Theory of Elasticity*, [Ed.] Arkady, Warszawa 1962, (in Polish).

*Received May 9, 2003
in revised form October 29, 2003*